03,09

# Non-steady-state photo-EMF in a periodically poled $MgO:LiNbO_3$ crystal

© M.A. Bryushinin[1], V.V. Kulikov[1], I.A. Sokolov[1], E.N. Savchenkov[2], N.I. Burimov[2], S.M. Shandarov[2], A.R. Akhmatkhanov[3], M.A. Chuvakova[3], V.Ya. Shur[3]

[1] Ioffe Institute,
St. Petersburg, Russia
[2] Tomsk State University of Control Systems and Radioelectronics,
Tomsk, Russia,
[3] Ural Federal University after the first President of Russia B.N. Yeltsin,
Yekaterinburg, Russia

E-mail: mb@mail.ioffe.ru

*Received November 3, 2022*
*Revised November 3, 2022*
*Accepted November 25, 2022*

The diffusion mode of the non-steady-state photo-EMF excitation is investigated in periodically poled $MgO:LiNbO_3$ crystal at light wavelength $\lambda = 457$ nm. The signal excitation is carried out along the polar axis of the crystal; the dependencies of the signal amplitude versus the phase modulation frequency, intensity and spatial frequency of the interference pattern are studied in this geometry. The analysis of these dependencies allows determining the photoelectric parameters of the material — the type, value and relaxation time of the photoconductivity, as well as the diffusion length of charge carriers.

**Keywords:** non-steady-state photo-EMF, periodic domain struc ture, lithium niobate.

DOI: 10.21883/PSS.2023.02.55400.519

## 1. Introduction

Periodically-poled lithium niobate has been already used in applied optics, but is still an object of interest for fundamental research as well. Thickness of walls separating the differently poled domains has an order of magnitude of the lattice constant and, therefore, investigation of charge transfer along such walls is as relevant as for carbon-based 2D structures that have become popular.

The experimental investigations of periodically-poled lithium niobate are primarily based on optical techniques, in particular, light diffraction [1,2]. Theoretical analysis of light beam propagation and holographic record herein has shown that an optically-induced change of the refraction index (optical damage) is reduced and holograms may be recorded at spatial frequencies determined by the combination of domain grating and recording interference pattern vectors [3,4]. Experimental investigations of the electrical properties of the material include conductivity measurements in individual domain walls and in domain walls array as well [5,6]. Among the optoelectronic techniques used before, investigation of non-steady-state photo-EMF effect in *single domain* $LiNbO_3$ should be noted, because it has facilitated determination of iron impurity center concentration and photovoltaic field [7]. Periodically-poled lithium niobate has not been investigated up to now.

The non-steady-state photo-EMF effect is observed in the form of alternating current occurring in a semiconductor when illuminated by an oscillating interference pattern [8]. The current is caused by periodic misalignment of photoconductivity and space charge field distributions. The effect is present in both centrosymmetric and non-centrosymmetric media. Semiconductor testing method based on this effect helps to determine the following parameters: type of conductivity and magnitude, charge carrier lifetime and diffusion length, and trapping center concentration [9,10]. The method was for the first time applied herein to a material with periodic domain structure — $MgO:LiNbO_3$ crystal.

## 2. Experimental setup

The non-steady-state photo-EMF experimental setup is shown in Figure 1. $\lambda = 457$ nm $P_{out} = 200$ mW single-frequency light is split into two beams, one of which is phase-modulated using an electrooptical modulator. The phase modulation amplitude is $\Delta = 0.36$. The beams are forwarded at a predefined angle to the test specimen, where an interference pattern is formed with average intensity $I_0$, contrast $m = 0.26$ and spatial frequency $K$. The laser emission polarization plane is perpendicular to the incidence plane. The current occurring in the crystal creates the appropriate voltage on load resistor $R_L = 1.0$ MΩ (100 kΩ for a frequency range up to 150 kHz). This voltage is amplified and measured by selective voltmeter. Current is calculated according to the crystal capacitance and preamplifier input capacitance $C_{cr} + C_{in} = 6.0$ pF.

Experiments on the same crystal $MgO:LiNbO_3$ are carried out herein as in [2]. The domain structure consists of wedge-shaped regions polarized in the opposite directions on the $z$ axis and alternating in the $x$ direction of the crystal with a period of 8.79 $\mu$m (Figure 1). Specimen dimensions are $8.0 \times 2.0 \times 1.0$ mm. The face and back

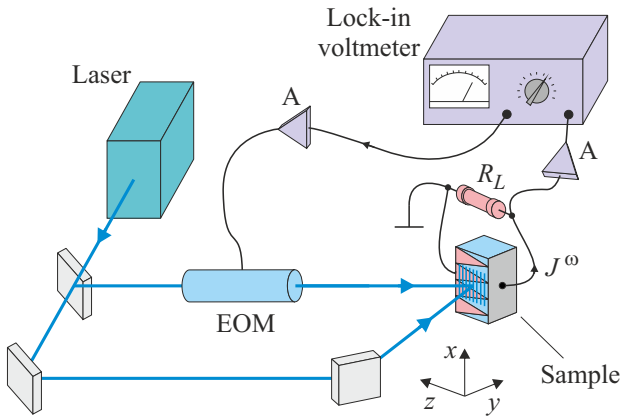


**Figure 1.** Non-steady-state photo-EMF effect experimental setup for $MgO:LiNbO_3$ crystal. *BS* — beamsplitter, *EOM* — electrooptical modulator, *M* — mirror.

$(8.0 \times 1.0\,\text{mm})$ have optical quality. Electrodes are applied to the sides $(8.0 \times 2.0\,\text{mm})$ using silver paste. The recorded grating vector and excited transient holographic current are parallel to the optical axis of the crystal.

## 3. Findings

Non-steady-state photo-EMF experiments are generally started with a relatively simple task — identify the phase of the signal to be detected and the type of material conductivity — *n*-type or *p*-type. In this $MgO:LiNbO_3$, the signal phase is of *n*-type conductivity.

Dependences of non-steady-state photo-EMF amplitude vs. light phase modulation frequency $\omega$, which is also interference pattern oscillation frequency, are shown in Figure 2. The dependence has growing, frequency-independent and declining segments. Such behavior is caused by change in charge grating oscillation amplitudes as the frequency increases. In the low frequency region, conductivity-band photo excited electron grating and space charge field grating formed on deep trapping centers track the interference pattern displacements. Spatial shift between the gratings is maintained at approx. $\pi/2$, which prevents the high drift current component to be achieved. As the frequency increases, the space charge field grating oscillation amplitude decreases — the grating becomes almost stationary. At the same time, the photoconductivity grating continues tracking the interference pattern displacement. Periodic misalignment of distributions increases causing a higher current amplitude. In the very high frequency band, both gratings become stationary, the resulting current decreases. The non-steady-state photo-EMF effect theory gives the following expression describing this signal behavior [9,10]:

$$J^\omega = \frac{-Sm^2(\Delta/2)\sigma_0 E_D i\omega\tau_M}{1-\omega^2\tau\tau_M + i\omega[\tau + \tau_M(1+K^2L_D^2)]}, \qquad (1)$$

where $S$ is the electrode area, $\sigma_0$ is the specific photoconductivity of the material, $E_D$ is diffusion field, $\tau_M = \epsilon\epsilon_0/\sigma_0$ is the Maxwell relaxation time [11], $\tau$ and $L_D$ is the electron lifetime and diffusion length, $\epsilon = 30$ is the permittivity, $\epsilon_0$ is the electric constant. Cut-off frequencies separating the frequency dependence segments are calculated as follows

$$\omega_1 = [\tau + \tau_M(1+K^2L_D^2)]^{-1}, \qquad (2)$$

$$\omega_2 = \omega_1 + (1+K^2L_D^2)/\tau. \qquad (3)$$

The signal dependence on light intensity is the essential characteristic of all photovoltaic phenomena, including also the non-steady-state photo-EMF effect (Figure 3). Linearity of $|J^\omega(I_0)|$ and $\omega_1(I_0)$ indicates the appropriate linearity of photoconductivity and electron recombination. This is also indicated by the relative independence of the second cut-off frequency on the light intensity: $\omega_2 \simeq \text{const}(I_0)$.

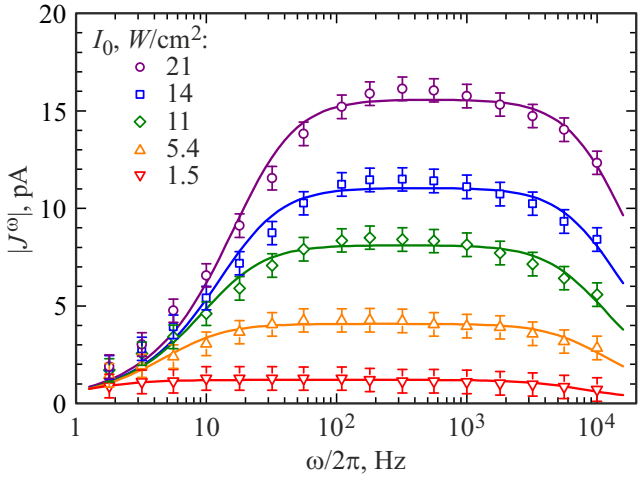


**Figure 2.** Frequency dependences of non-steady-state photo-EMF amplitude measured at different light intensities $K = 1.6\,\mu\text{m}^{-1}$.

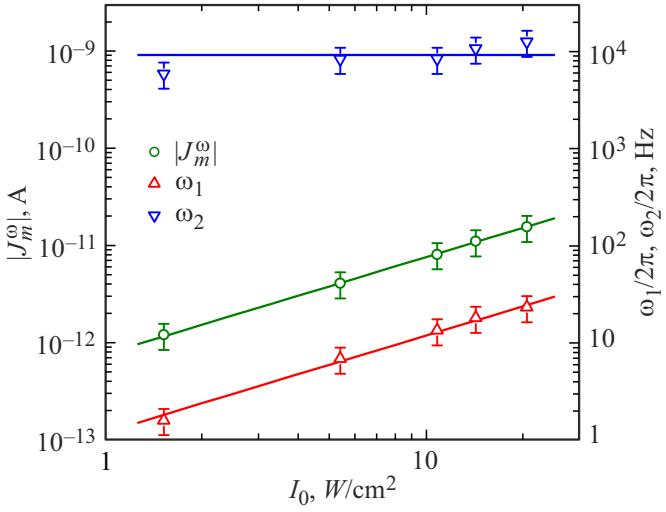


**Figure 3.** Dependence of maximum non-steady-state photo-EMF amplitude and cut-off frequencies vs. light intensity. $K = 1.6\,\mu\text{m}^{-1}$.

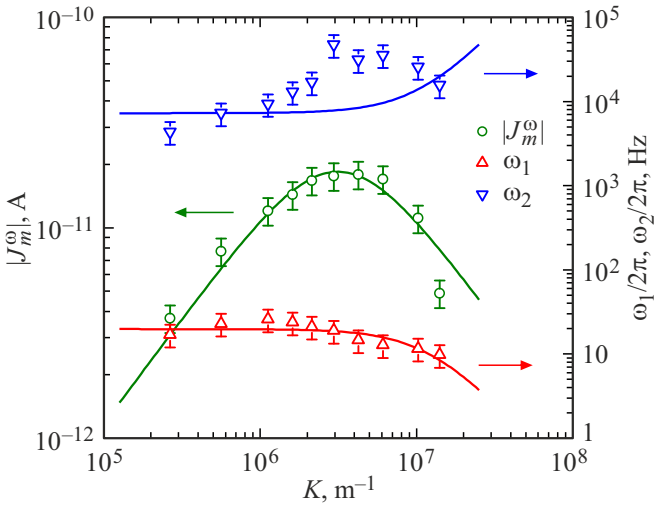


**Figure 4.** Dependences of the maximum non-steady-state photo-EMF amplitude and cut-off frequencies vs. interference pattern spatial frequency. $I_0 = 21\,\mathrm{W/cm^2}$.

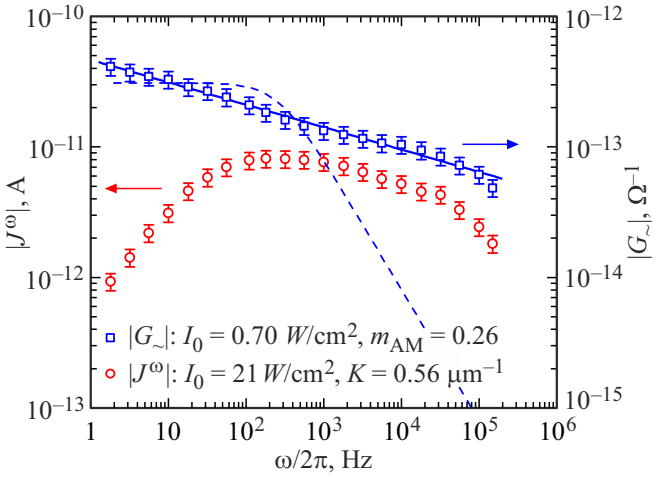


**Figure 5.** Frequency dependences of non-steady-state photo-EMF amplitude and photoconductivity response amplitude. For dependence $|G(\omega)|$, approximation with standard expression $|1 + i\omega\tau|^{-1}$ and power function $\omega^{-0.17}$ is shown.

Without external electrical field, the space charge field grating amplitude is defined by the diffusion field magnitude which, in turn, depends on the spatial frequency: $E_D = (k_B T/e)K$, where $k_B$ is the Boltzmann constant, $T$ is the crystal temperature, $e$ is the elementary charge. It is obvious that the current resulting from the photoconductivity and field grating interaction shall be also the spatial frequency function. This dependence was measured experimentally (Figure 4). Current amplitude decrease in the high space frequency band is attributed to diffusive „spreading" of the oscillating photoconductivity grating component. Signal maximum is achieved at spatial frequency $K = L_D^{-1}$. This feature is used for calculating charge carrier diffusion length: $L_D = 0.32\,\mu$m for $MgO:LiNbO_3$ of interest.

Cut-off frequencies $\omega_1$, $\omega_2$ in low $K$ region are defined only by characteristic times $\tau_M$ and $\tau$, which is also used for determining photoelectric parameters. For high-resistance materials, generally $\tau_M \gg \tau$, therefore $\omega_1 \simeq \tau_M^{-1}$ and $\omega_2 \simeq \tau^{-1}$. From dependences in Figure 4, find $\tau_M = 8.0\,$ms and $\tau = 22\,\mu$s. Specific photoconductivity is $\sigma_0 = 3.3 \cdot 10^{-10}\,\Omega^{-1}\mathrm{cm}^{-1}$ at light intensity $I_0 = 21\,\mathrm{W/cm^2}$.

Dependence $\omega_2(K)$ in Figure 4 considerably differs from the theoretical dependence, therefore non-steady-state photo-EMF and photoconductivity response are measured in amplitude-modulated light in the extended frequency band (Figure 5). Similarity of dependences in $0.1-100\,$kHz band indicates that the non-steady-state photo-EMF is associated with the photoconductivity relaxation. Both dependences demonstrate abnormal behavior: instead of the expected signal amplitude decline in inverse proportion to frequency, $|J^\omega(\omega)|$, $|G_\sim(\omega)| \propto \omega^{-0.17}$ are observed. In this case, it is problematic to determine cut-off frequency $\omega_2$ and time $\tau$ from the experimental curves. Specimen resistance can be assessed from $|G_\sim(\omega)|$ as follows: $R_0 = G_0^{-1} = (G_\sim(0)/m)^{-1} = 630\,\mathrm{G\Omega}$ for $I_0 = 0.7\,\mathrm{W/cm^2}$. Specific photoconductivity equivalent to the experiment intensity level with non-steady-state photo-EMF ($I_0 = 21\,\mathrm{W/cm^2}$) is equal to $2.4 \cdot 10^{-10}\,\Omega^{-1}\mathrm{cm}^{-1}$.

## 4. Discussion of findings

Non-steady-state photo-EMF signal behavior in periodically-poled $MgO:LiNbO_3$ is well described within standard effect theory [8] in rather wide phase modulation frequency band ($10^0 - 10^4\,$Hz). Though the lithium niobate crystal is known for its photovoltaic properties, no direct manifestation of these properties in the effect of interest has been found. The first reason of this is the process reason: magnesium oxide doping of crystal reduces the photovoltaic field and, thus, allows to reduce the optical damage of specimens. Formation of periodic domain structure also reduces the averaged photovoltaic field and the related change in the light refraction index [3].

Doping and periodic structure formation do not eliminate the photovoltaic effect completely, therefore we will try to assess its contribution to the non-steady-state photo-EMF effect. The main equation describing the space charge field formation in photorefractive crystals is written as follows [11]:

$$\frac{\partial E_{sc}}{\partial t} = -\frac{m(iE_D + E_0 + E_G) + E_{sc}}{\tau_M(1 + K^2 L_D^2 - iKL_0)}, \qquad (4)$$

where $E_{sc}$ is the complex amplitude of the electric space charge field strength, $L_0$ is the drift length, $E_0$ is the external electric field strength, $E_G$ is the photovoltaic field. Using this equation, the expression was obtained in [8] for complex amplitude of non-steady-state photo-EMF excited in the

external field without photovoltaic effect ($E_0 \neq 0$, $E_G = 0$):

$$j^{\omega} = \frac{m^2\Delta}{4}\sigma_0\left[\frac{i2E_0 - \omega\tau_M(iE_D + E_0)}{1 + i\omega\tau_M(1 + K^2L_D^2 + iKL_0)} + \frac{-i2E_0 - \omega\tau_M(iE_D - E_0)}{1 + i\omega\tau_M(1 + K^2L_D^2 - iKL_0)}\right]. \quad (5)$$

Similarly to equation (4), replace $E_0$ with $E_0 + E_G$ in (5). Then, by assuming the external field to be equal to zero, the following expression for our case ($E_0 = 0$, $E_G \neq 0$) is derived:

$$j^{\omega} = \frac{m^2\Delta}{2}\sigma_0 E_D \frac{-i\omega\tau_M}{1 + i\omega\tau_M(1 + K^2L_D^2)}. \quad (6)$$

This expression contains no photovoltaic contribution and precisely meets the diffusion excitation case ($E_0, E_G = 0$). This supports the test findings with periodically-poled $MgO:LiNbO_3$, where no any photovoltaic effect occurs. It should be noted that the shown derivation of expression (6) from expressions (4) and (5) is not rigorous, photovoltaic effect influence on the non-steady-state photo-EMF excitation process will be probably detected by in-depth theoretical consideration of the effect.

It is generally believed that electrical conductivity in $LiNbO_3$ is implemented by means of polaron and hopping charge transfer [12,13]. This is, in particular, indicated by the time-stretched relaxation of various physical quantities such as charge carrier and charged center concentrations, light absorption factor. Such relaxation is well described by so called KWW function (Kohlrausch–Williams–Watts): $f(t) = \exp[-(t/\tau)^{\beta}]$, where $0 < \beta < 1$ [12–14]. Stretched exponent has an equivalent describing the frequency band processes, — HN-function (Havrliliak–Negami):

$$f(\omega) = [1 + (i\omega\tau)^{\alpha}]^{-\gamma}. \quad (7)$$

where $0 < \alpha \leq 1$, $\gamma > 0$ and $\alpha\gamma \leq 1$. The power function used by us for approximation of $|G(\omega)|$ in Figure 5, can be considered as a part of HN-function with $\alpha\gamma = 0.17$ and $\omega\tau \gg 1$. The causes of such non-Debye relaxation in $LiNbO_3$ have not been finally found, empirical approach to this problem suggests that the observed dependences are a combination of multiple relaxation processes with various time constants $\tau$ [13].

It should be noted that the obtained photovoltaic parameter values are averaged by domain structure period. An effort was made to detect the effect periodicity with crystal displacement in the $x$ direction and illumination with interference pattern focused using a cylindrical lens into a narrow stripe parallel to the $z$ axis. If the effort is successful, it would allow to assess the relative contributions of the domain volumes and domain walls to the signal amplitude and appropriate photoelectric parameters. Unfortunately the specified periodicity was not detected. Most probably this is attributed to the fact that no sufficiently thin waists of light beams ($\sim 1-3\,\mu$m) can be obtained throughout the crystal thickness (2 mm). The use of thin specimens is an obvious solution of the problem and is considered as a direction for future experimental investigations.

## 5. Conclusion

Excitation of non-steady-state photo-EMF in the periodic domain structure based on $MgO:LiNbO_3$ crystal was performed herein for the first time. The signal demonstrated the behavior typical of diffusion mode of charge grating recording. The review of the measured dependences of the signal vs. illumination parameters has shown satisfactory compatibility with the effect theory developed earlier for common semiconductor materials without photovoltaic effect and periodic domain structure. On frequency dependences of non-steady-state photo-EMF and photoconductivity response, a slow signal decline segment was found. The segment is typical of polaron and hopping charge transfer in $LiNbO_3$. Photoelectric parameters of the material were determined for light wavelengths $\lambda = 457$ nm.

## Funding

This study was funded by the Ministry of Science and Higher Education of the Russian Federation within the framework of the state order for 2020-2022 (job-order FEWM-2020-0038/3). The study was performed using the equipment provided by Ural Common Use Center „Modern Nanotechnologies“ Ural Federal University (Reg. No. 2968) supported by the Ministry of Science and Higher Education of the Russian Federation (project 075-15-2021-677).

## Conflict of interest

The authors declare that they have no conflict of interest.

## References

[1] M. Müller, E. Soergel, K. Buse, C. Langrock, M.M. Fejer. J. Appl. Phys. **97**, *4*, 044102 (2005).
[2] E.N. Savchenkov, A.V. Dubikov, D.E. Kuzmich, A.E. Sharaeva, S.M. Shandarov, N.I. Burimov, M.A. Chuvakova, A.R. Akhmatkhanov, V.Y. Shur. Opt. Mater. **122**, B, 111813 (2021).
[3] M. Taya, M.C. Bashaw, M.M. Fejer. Opt. Lett. **21**, *12*, 857 (1996).
[4] B. Sturman, María Aguilar, F. Agulló-López, V. Pruneri, P.G. Kazansky. J. Opt. Soc. Am. B **14**, *10*, 2641 (1997).
[5] M. Schröder, A. Haußmann, A. Thiessen, E. Soergel, T. Woike, L.M. Eng. Adv. Funct. Mater. **22**, *18*, 3936 (2012).
[6] C.S. Werner, S.J. Herr, K. Buse, B. Sturman, E. Soergel, C. Razzaghi, I. Breunig. Sci. Rep. **7**, 9862 (2017).
[7] H. Veenhuis, K. Buse, E. Krätzig, N. Korneev, D. Mayorga. J. Appl. Phys. **86**, *5*, 2389 (1999).
[8] M.P. Petrov, I.A. Sokolov, S.I. Stepanov, G.S. Trofimov. J. Appl. Phys. **68**, *5*, 2216 (1990).

[9] S. Stepanov. In: Handbook of advanced electronic and photonic materials and devices, v. 2: Semiconductors devices / Ed. H.S. Nalwa. Academic Press, Burlington (2001). P. 205.
[10] I.A. Sokolov, M.A. Bryushinin. Optically induced space-charge gratings in wide-bandgap semiconductors: techniques and applications. Nova Science Publishers, Inc., N.Y. (2017). 229 p.
[11] M.P. Petrov, S.I Stepanov, A.V. Khomenko. Fotorefraktivnyie krictally v kogerentnoy optike. Nauka, SPb. (1992). 320 p. (in Russian).
[12] B. Sturman, M. Carrascosa, F. Agullo-Lopez. Phys. Rev. B **78**, *24*, 245114 (2008).
[13] M. Imlau, H. Badorreck, C. Merschjann. Appl. Phys. Rev. **2**, *4*, 040606 (2015).
[14] B. Sturman, E. Podivilov, M. Gorkunov. Phys. Rev. Lett. **91**, *17*, 176602 (2003).

*Translated by Ego Translating*